Multiscale and Multidisciplinary Modeling, Experiments and Design (2024) 7:395–409
https://doi.org/10.1007/s41939-023-00219-z

ORIGINAL PAPER

Neuro-fuzzy system development to estimate the compressive strength of improved high-performance concrete

Zhiqiang Niu[1] · Yan Yuan[1] · Jianglan Sun[1]

Received: 19 June 2023 / Accepted: 1 August 2023 / Published online: 21 August 2023

Abstract

High-performance concrete (HPC) outperforms regular concrete due to incorporating additional components that go beyond the typical ingredients used in standard concrete. Various artificial analytical methods were employed to assess the compressive strength (CS) of high-performance concrete containing fly ash (FA) and blast furnace slag (BFS). The primary objective of this study was to present a practical approach for a comprehensive evaluation of machine learning algorithms in predicting the CS of HPC. The study focuses on utilizing the adaptive neuro-fuzzy inference system (ANFIS) to develop models for predicting HPC characteristics. To enhance the performance of ANFIS methods, the study incorporates the arithmetic optimization algorithm (AOA) and equilibrium optimizer (EO) (abbreviated as ANAO and ANEO, respectively). Notably, this research introduces novelty through the application of the AOA and EO, the evaluation of HPC with additional components, the comparison with prior literature, and the utilization of a large dataset with multiple input variables. The results indicate that the combined ANAO and ANEO systems demonstrated strong estimation capabilities, with R^2 values of 0.9941 and 0.9975 for the training and testing components of ANAO, and 0.9878 and 0.9929 for ANEO, respectively. The results comparison of this study presented the comprehensiveness and reliability of the created ANFIS model optimized with AOA for predicting the HPC's CS improved with FA and BFS, which could be applicable for practical usages.

Keywords High-performance concrete · Compressive strength · Prediction · Adaptive neuro-fuzzy inference system · Optimization algorithms

1 Introduction

High-performance concrete (HPC) elements have found widespread application in structures such as large bridges, tall buildings, and dams, known for their exceptional performance (Esmaeili-Falak et al. 2018). Commonly included in the mixture are fly ash, blast furnace slag, and supplementary additives like super-plasticizers (Neville and Aitcin 1998; Leung 2001). The proportions of each ingredient can be adjusted to achieve desired efficiency and strength objectives (Pala et al. 2007). Due to the inherent non-homogeneity of concrete mixes, determining the appropriate mixing ratios and accurately predicting the compressive strength (CS) of concrete poses a challenge. As a result, there has been considerable focus on employing machine learning (ML) techniques to minimize the disparity between predicted and observed outcomes. In the past 20 years, a range of machine learning methodologies has been utilized to develop precise and efficient solutions for predicting the CS of HPC and other related fields. Artificial neural networks (ANNs) with fuzzy style (Kasperkiewicz et al. 1995), and multi-layer (Sarıdemir 2009; Lee 2003; Esmaeili-Falak et al. 2019; Aghayari Hir et al. 2022) are the two most popular types, along NN with single layer (Lai and Serra 1997) and multi-layer (Najafzadeh and Azamathulla 2015; Najafzadeh et al. 2018; Najafzadeh and Saberi-Movahed 2019).

Yeh (1998a, 2006) provided a laboratory dataset of 1030/1133 individual tests conducted on HPC. The dataset included eight dependent parameters and one independent parameter (i.e., CS), representing the mixing percentages. Additional ML techniques that can be employed to forecast the properties of HPC encompass support vector machine (SVM) (Rafiei et al. 2017; Yan and Shi 2010; Wu and Zhou 2022a), computational ensemble approaches such as random

✉ Zhiqiang Niu
oxok815@163.com

[1] Faculty of Civil and Architectural Engineering, Zhengzhou University of Science and Technology, Zhengzhou 450064, China

forest (RF) (Han et al. 2019; Dawei et al. 2023), boosting smooth transition regression trees (Anyaoha et al. 2020; Zhu et al. 2022) or other methods (Wu and Zhou 2022b; Benemaran 2023). Some researchers have explored the combination of ANNs with fuzzy logic (Topcu and Sarıdemir 2008; Zarandi et al. 2008; Masoumi et al. 2020), regression analysis (Atici 2011), or a variety of algorithms including SVM, ANNs, and linear regression (Chou and Pham 2013; Chou and Tsai 2012). Young et al. (Young et al. 2019) employed NN, gradient boosting (GB), RF, and SVM models to predict the CS of over 10,000 specimens. The study aimed to incorporate the actual mixtures and consider their industrial significance. Newer publications (Asteris et al. 2021; Nguyen et al. 2021a) provide insights into ML models that are often referred to as black box techniques. These models do not explicitly reveal the process of combining inputs to generate forecasts, yet they offer advantages such as high sensitivity, simplicity, and robustness. Due to the lack of a clear correlation between the CS and the input variables, utilizing them poses a significant challenge. To address this issue, various intricate mathematical theories have been developed to establish a connection. Yeh and Lien (2009) introduced a genetic operation tree approach that combined an operation tree with a genetic method to compute the CS. Capitalizing on the advantages of ANNs, researchers have integrated them with genetic programming (GEP) (Chopra et al. 2016; Baykasoğlu et al. 2004) or fuzzy logic (Akkurt et al. 2004). However, it is worth mentioning that the detailed equations utilized in the mathematical formulations presented in these articles might be intricate and demanding to grasp. Linear, non-linear, and meta-heuristic regression approaches (Le-Duc et al. 2020; Chou et al. 2016) leverage the correlation coefficients of the factor percentages to predict the CS. These diverse approaches offer various methods for estimating CS. Bharatkumar et al. (2001) explored the impact of water content and mineral additions on the mixture design method of HPC. Bhanja and Sengupta (2002) identified the correlation between water-to-cement (W/C) ratio, silica fume (SF) substitution rates, and the CS. Namyong et al. (2004) developed a regression method to predict the CS of conventional concrete. Zain and Abd (2009) aimed to forecast the strength of HPC using a multiple non-linear regression approach. Considering that laboratory samples may involve errors in the combination percentages and testing procedures, it becomes crucial to incorporate unknown factors into the classification algorithm (Young et al. 2019). The adaptive neuro-fuzzy inference system (ANFIS) offers several advantages, including flexibility, universal approximation, and learning capability (Campo et al. 2011; Mittal et al. 2011; Chen et al. 2018). ANFIS enables the generation of flexible rules and the modeling of complex systems using linguistic variables and if–then rules. This makes it particularly suitable for domains where interpretability is crucial. ANFIS possesses the capability to approximate continuous functions with high precision. It employs a hybrid learning algorithm that merges gradient descent and least-squares estimation. This unique approach allows ANFIS to learn from data and optimize its parameters, rendering it suitable for a wide range of learning tasks, both supervised and unsupervised. Modern optimization algorithms utilize advanced search strategies and mechanisms to enhance both exploration and exploitation of the search space. Unlike older evolutionary optimizers, which may face difficulties in handling complex optimization problems characterized by high-dimensional search spaces, non-linear relationships, constraints, or multimodal landscapes, novel optimization algorithms are specifically designed to tackle such challenges. These new algorithms often incorporate mechanisms to improve robustness in the presence of noise or uncertainty in problem environments. Moreover, many novel optimization methods offer a high level of customization and flexibility, allowing them to be adapted to various problem domains (Sarkhani Benemaran et al. 2020; Esmaeili-Falak and Hajialilue-Bonab 2012; Moradi et al. 2020).

The primary objective of this study is to present a practical approach for a comprehensive evaluation of machine learning algorithms in predicting the CS of HPC. The study focuses on utilizing the ANFIS to develop models for predicting HPC characteristics. To enhance the performance of ANFIS methods, the study incorporates the arithmetic optimization algorithm (AOA) and Equilibrium optimizer (EO), using a dataset of 1030 test samples, 8 input parameters, and CS as the target prediction variable. The obtained results are then compared with existing literature findings. Notably, this research introduces novelty through the application of the AOA and EO, the evaluation of HPC with additional components, the comparison with prior literature, and the utilization of a large dataset with multiple input variables. These aspects contribute to advancing the understanding of predicting mechanical properties in HPC and provide a fresh approach for optimizing the performance of predictive models.

The innovativeness of this paper lies in several aspects:

- The researchers introduce and apply two optimization algorithms, namely the AOA and the EO, to enhance the performance of the ANFIS for predicting the CS of HPC. These algorithms may not have been widely used in this specific context before, and their incorporation demonstrates the potential for improving the accuracy of the predictive models.
- Evaluating the CS of HPC with these additional components adds novelty to the research, as it explores how different ingredients impact the concrete's properties. This examination is crucial in understanding how to optimize HPC for specific applications.

Table 1 The value of statistical indices of inputs and goal

Data	Index	Inputs								Output
		C (kg/m^3)	$\frac{W}{C}$	$\frac{FA}{C}$	$\frac{BFS}{C}$	$\frac{CAG}{C}$	$\frac{FAG}{C}$	AC (days)	$\frac{SP}{C}$	CS (MPa)
Trainingphase	Minimum	102	0.267	0.0	0.0	1.552	1.226	3.0	0.0	2.332
	Maximum	540	1.882	1	1.504	8.696	9.235	365.000	0.069	82.599
	Standarddviation	101.84	0.298	0.306	0.446	1.549	1.323	67.717	0.02	17.718
	Skewness	0.511	1.163	0.989	1.467	0.596	1.194	2.993	0.245	0.304
	Kurtosis	− 0.692	2.104	− 0.269	1.284	− 0.127	2.572	10.189	− 1.243	− 0.549
Testingphase	Minimum	132	0.2	0.0	0.0	1.716	1.135	1.0	0.0	6.267
	Maximum	540	1.694	1.430	1.584	7.148	5.993	360	0.125	74.987
	Standarddviation	110.075	0.341	0.418	0.513	1.632	1.405	50.155	0.031	13.44
	Skewness	0.533	0.554	1.043	1.036	0.580	0.556	4.229	0.873	0.499
	Kurtosis	− 0.228	− 1.068	− 0.307	− 0.314	− 1.237	− 0.956	20.129	0.190	0.214

– The primary objective of the research is to provide a practical approach for comprehensively evaluating machine learning algorithms for predicting the c CS of HPC. While ANFIS is used as the main algorithm, the paper might explore and discuss the results obtained from other machine learning algorithms as well, contributing to a broader understanding of their effectiveness in this specific domain.
– The paper emphasizes the practical usages of the developed ANFIS models optimized with AOA and EO for predicting the CS of HPC improved with fly ash and blast furnace slag. By demonstrating the models' effectiveness for real-world applications, the study provides actionable insights that can be directly implemented in the construction industry.

2 Methodology

2.1 Data

Larger than 1000 HPC specimens, which were applied in publications (Dawei et al. 2023; Anyaoha et al. 2020; Zhu et al. 2022; Wu and Zhou 2022b; Benemaran 2023), have been evaluated in this study (Yeh 2006, 1998a, b, 1999, 2003). All the instances were created using ordinary Portland cement (OPC) and were then left to dry naturally. So far, the existing literature on HPC testing data has employed various types and sizes of samples. The compressive strength of HPC is determined based on eight variables: cement content (C), blast furnace slag to cement ratio (BFS/C), fly ash to cement ratio (FA/C), water-to-cement ratio (W/C), superplasticizer to cement ratio (SP/C), coarse aggregate to cement ratio (CAG/C), fine aggregate to cement ratio (FAG/C), and the curing time of HPC (AC). In the database, Table 1 illustrates the ranges of these components, while Fig. 1 exhibits the distribution graphs for both the training and testing datasets.

The dataset consisting of 1030 entries was divided into two sets: the training set accounted for 70% of the data, while the remaining 30% constituted the testing set. The selection of these subgroups from the source data was done randomly using a uniform distribution (Sarkhani Benemaran et al. 2022). Although previous publications (Leema et al. 2016; Khorsheed and Al-Thubaity 2013) suggested using various other train/test ratios, a 70/30 ratio for training/testing groups was employed in this investigation. The range of all input variables was found to be extensive. Through statistical analysis, it was demonstrated that the selection of these input variables was appropriate, as no significant overlap was observed in the eight-dimensional input space (Yeh 2006, 1998a, b, 1999, 2003). This is crucial for training AI systems with robust generalization capabilities.

Researchers utilized Eq. (1) to apply the Pearson correlation coefficient (P_{CC}):

$$\sigma_{y,z} = \frac{\mu(y, z)}{\delta_y \delta_z}. \tag{1}$$

In Eq. (1), $\mu(y, z)$, δ_y, and δ_z show the covariance between y and z, the standard deviation of y, and the standard deviation of z. The P_{CC} values between the input and output parameters are depicted in Fig. 2. If there are significant positive or negative influences from P_{CC} that play a major role, the study's failure to clarify the impact of these influences on the results might indicate a deficiency in the methodology employed. Several P_{CC} values were below 0.531, suggesting that these particular values are unlikely to be the primary source of the multicollinearity issues. The interplay between

Fig. 1 The distribution of the variables

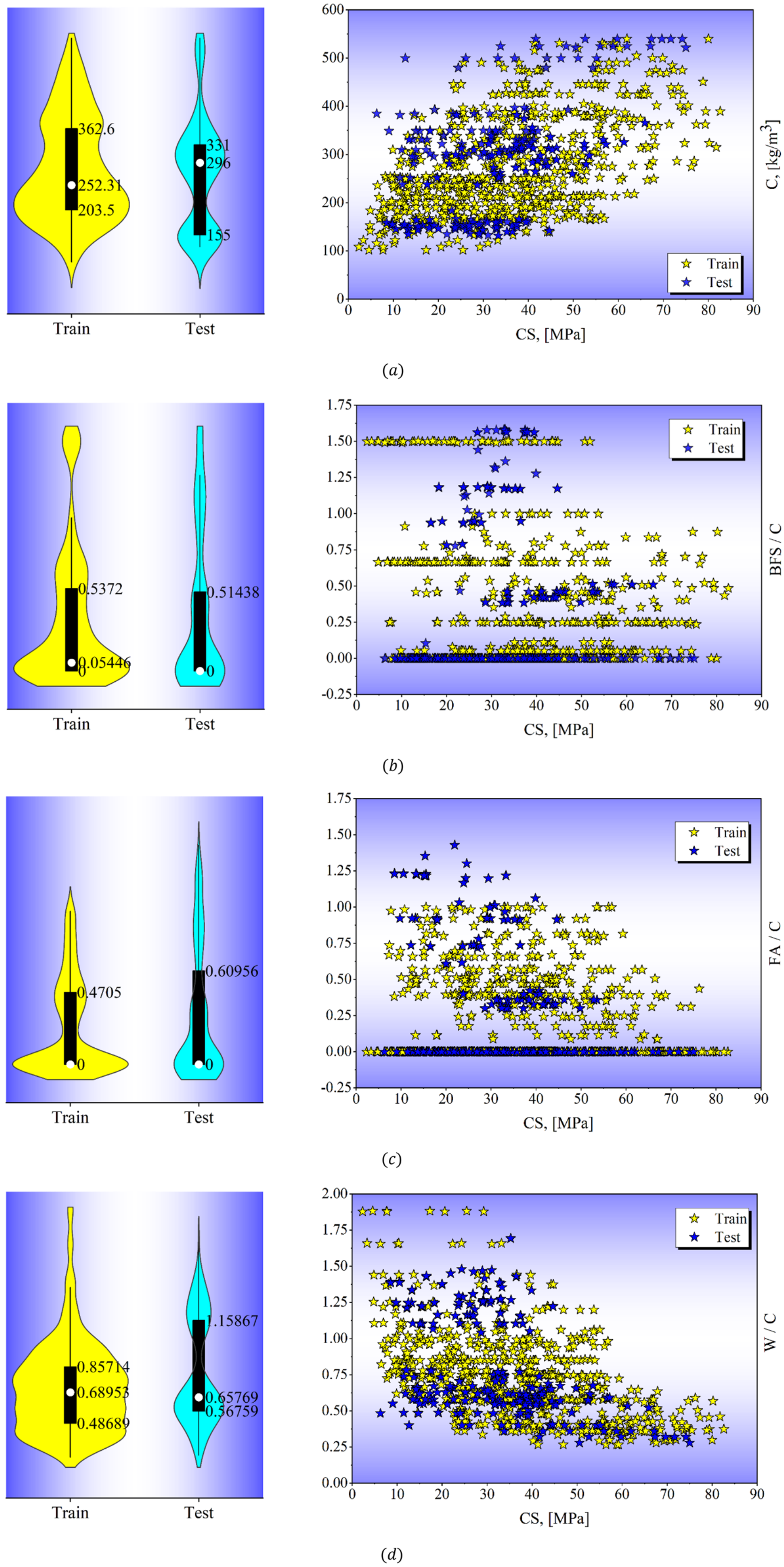

Fig. 1 continued

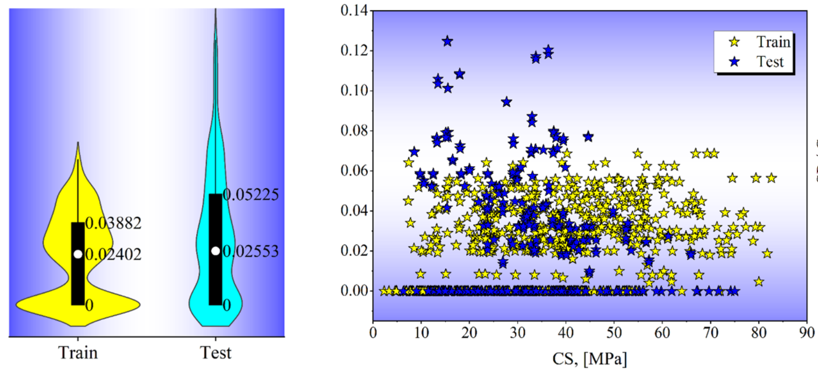

(*e*)

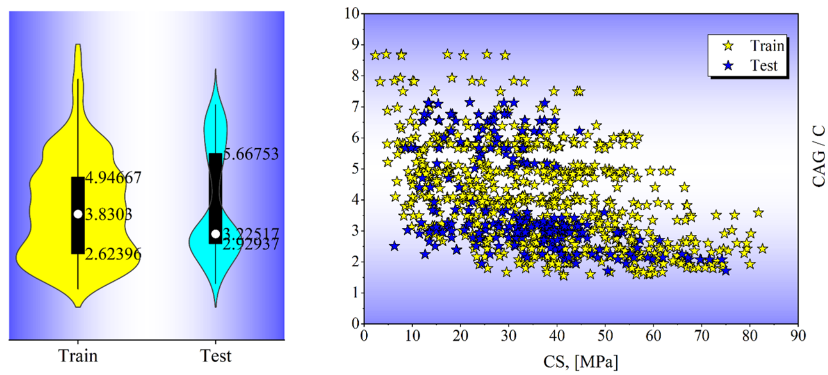

(*f*)

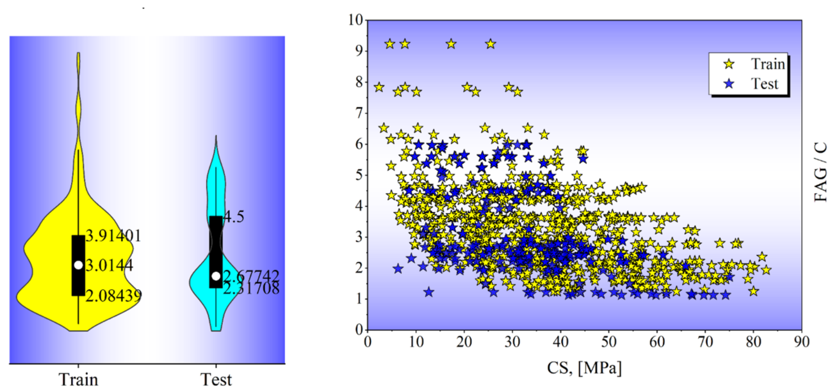

(*g*)

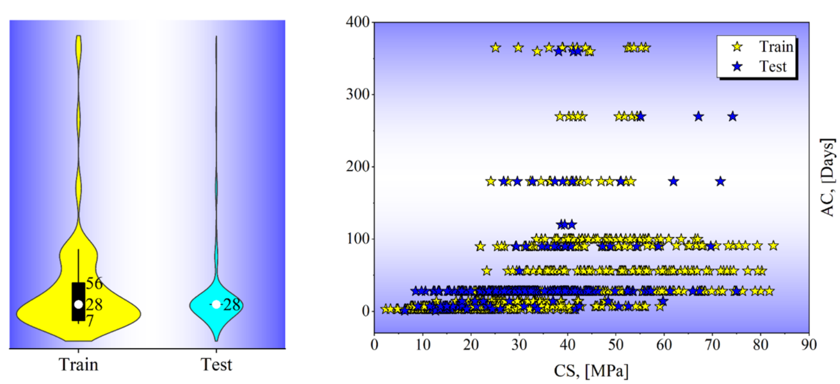

(*h*)

Fig. 2 P_{CC} matrix

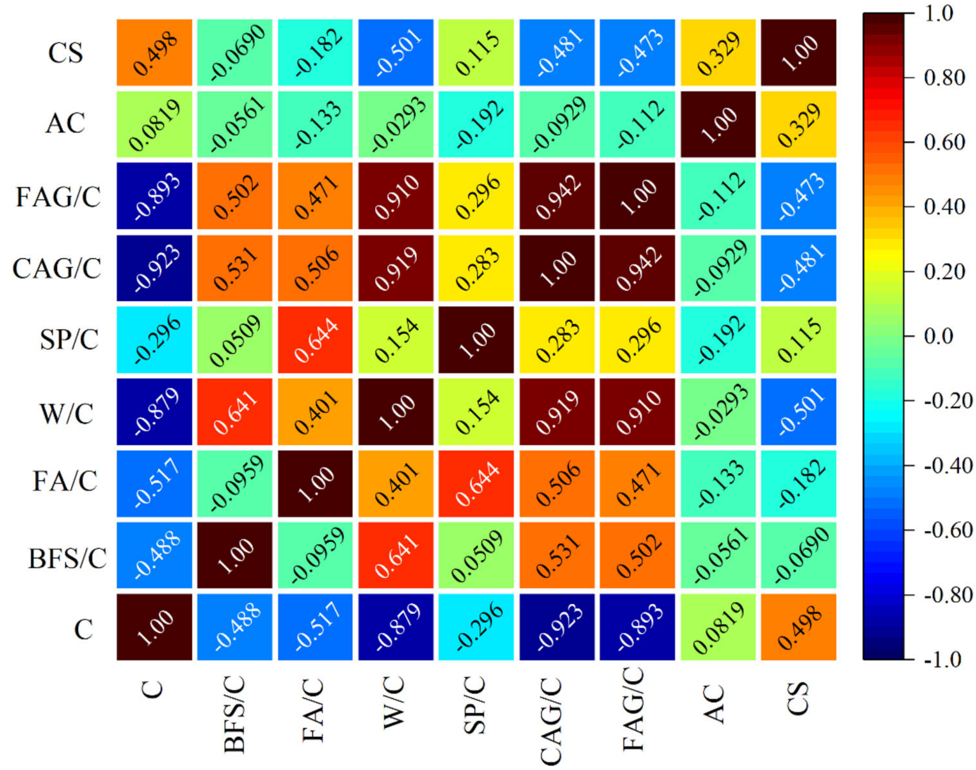

various variables is evident, with significant mutual influences observed (above a threshold of 0.641). The strongest correlation, at a value of 0.942, is observed between CAG$/C$ and FAG$/C$. In addition, there are notable negative correlations that may pose challenges during the prediction process. The most pronounced adverse associations are found between C and CAG$/C$, with a correlation of -0.923.

2.2 Applied methods

2.2.1 Arithmetic optimization algorithm (AOA)

A novel meta-heuristic approach called the AOA was put out in 2021 (Abualigah et al. 2021). As suggested by the name, the location updating formulas for finding the universal optimization answer represent four conventional arithmetic operators: multiplication operator (M), division operator (D), addition operator (A), and subtraction operator (S). The multiplication (M) and division (D) are employed for the exploratory search, providing enormous steps in the search area based on the various impacts of these four arithmetic operators. In addition, the exploitation search—which may produce tiny stage sizes in the search space—is executed using the addition (A) and subtraction (S) operations. Figure 3 displays the AOA's thorough optimization method.

The mathematical formulas for exploration and exploitation manners are given by the subsequent formulae, as shown in Fig. 3:

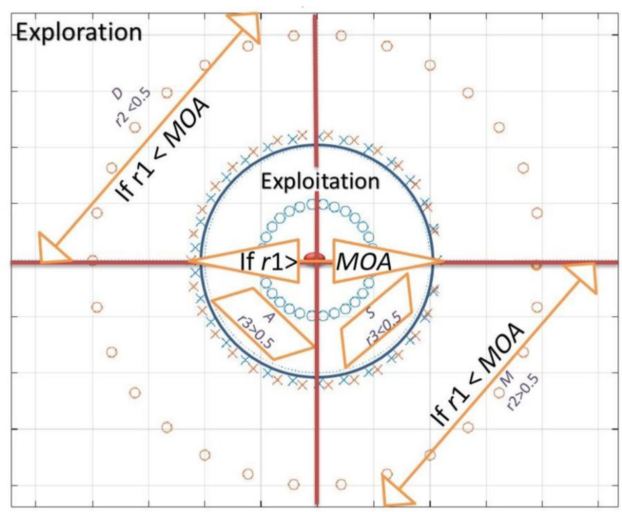

Fig. 3 Location updating procedure of search agents in AOA and impacts of MOA on it (Abualigah et al. 2021)

$$X_i(t+1) = \begin{cases} X_b(t) \div (\mathrm{MOP} + \mathrm{eps})((\mathrm{UB} - \mathrm{LB}) \\ \quad \times \mu + \mathrm{LB}), \ \mathrm{rand} < 0.5 \\ X_b(t) \times \mathrm{MOP} \times ((\mathrm{UB} - \mathrm{LB}) \times \mu + \mathrm{LB}), \ \mathrm{rand} \geq 0.5 \end{cases}, \tag{2}$$

$$X_i(t+1) = \begin{cases} X_b(t) - \mathrm{MOP} \times \\ ((\mathrm{UB} - \mathrm{LB}) \times \mu \\ + \mathrm{LB}), \ \mathrm{rand} < 0.5 \\ X_b(t) + \mathrm{MOP} \times ((\mathrm{UB} - \mathrm{LB}) \\ \times \mu + \mathrm{LB}), \ \mathrm{rand} \geq 0.5 \end{cases}. \tag{3}$$

Based on these equations, the recently produced location is denoted by $X_i(t+1)$. And in the tth iteration, search factors discovered the optimal spot at $X_b(t)$. To guarantee the dividend is positive, eps is a very modest positive value. A constant coefficient is μ. The upper and lower border are denoted by UB and LB. A random number evenly divided between 0 and 1 is called "rand". A crucial non-linear coefficient dropped from 1 to 0 simultaneously with the iterations is the math optimizer probability (MOP). Moreover, here is the MOP computation expression:

$$\mathrm{MOP} = 1 - \left(\frac{t}{T}\right)^{\frac{1}{\alpha}}. \tag{4}$$

In Eq. (4), α stands for the constant that is fixed as 5 in AOA, and T denotes the iterations' highest number.

The math optimizer accelerated (MOA) used to balance exploration, and exploitation is also a crucial AOA parameter. The MOA is determined using the following equation:

$$\mathrm{MOP}(t) = \mathrm{Min} + t \times \left(\frac{\mathrm{Max} - \mathrm{Min}}{T}\right). \tag{5}$$

Based on this equation, Max and Min show the MOA's highest and lowest values. When the AOA begins to function, the exploration search—that is, multiplication (M) or division (D)—will be chosen and carried out if a random integer (among 0 and 1) is larger than the MOA. If not, the addition (A) or subtraction (S) exploitation search will be carried out. The likelihood of local searches by search factors will rise as the number of iterations rises. In Algorithm 1, the pseudo-code for AOA is displayed.

Algorithm 1. The AOA's Pseudocode [56]

Initialization

Initialize the population size (N) and the number of iterations (T)

Initialize the positions of all search agents X_i $(i = 1, 2, 3, \ldots, N)$

Evaluate the fitness of search agents and find the current best position and best Fitness, X_b

Set the parameters α, μ, Min and Max

Main loop {

While $(t \leq T)$

Calculate the MOP by Eq (4)

Calculate the MOA by Eq (5)

For each search agent

If $rand > MOA$

Update position by Eq (2)

Else

Update position by Eq (3)

End if

Calculate the fitness of the search agent

Update current best position and best Fitness, X_b

End for

t = $t + 1$

End While}

Return the best Fitness, X_b

2.2.2 Equilibrium optimizer (EO)

As mentioned in Faramarzi et al. (2020), EO is a new and potential method since it produces outputs that are more precise than those of previous methods. In order to obtain the ideal hub heights for the wind turbines, it will be used here.

Control volume mass balance models are the foundation of EO. It is used to calculate the equilibrium and dynamic states in that each particle's concentration serves as a search factor. To achieve the optimal outcome (equilibrium state), the concentrations, as given in Eq. (6), are arbitrarily updated for every search agent about the optimal answers (equilibrium options):

$$\mathrm{CON} = \mathrm{COeq} + (\mathrm{CON1} - \mathrm{COeq}) \times f + \frac{g}{\lambda \times vo}(1 - f). \tag{6}$$

Based on this equation, f denotes an exponential term, CON1 represents the beginning concentration, g indicates the mass generation level, λ stands for the turnover level, and vo defines the control volume. COeq is the concentration in the equilibrium state.

The following three steps (Faramarzi et al. 2020) may be used to briefly summarize the EO method:

- Initializing and assessing the function which starts the population is the first stage. Equation (7), which describes the initialization in the observed area using a standard arbitrary initialization, depends on the dimensions and particle counts. $C\mathrm{in}_j$ stands for the particle j's concentration vector, $C\mathrm{min}$ for the dimension's lowest value and $C\mathrm{max}$ for its highest value, and rand_j for the particle j's random vector, where k is the particles count:

$$C\mathrm{in}_j = C\mathrm{min} + \mathrm{rand}_j(C\mathrm{max} - C\mathrm{min}) \quad \text{for } j = 1, 2, \ldots, K. \tag{7}$$

- The equilibrium pool and the options chosen from the population are covered in the second stage. In addition to the particle with the mean of the finest parts, the top four equilibrium options are also utilized. Using these five equilibrium possibilities, as shown in Eq. (8), the exploration and exploitation phases may be enhanced:

$$C\mathrm{pool} = \left[\mathrm{COeq1}, \mathrm{COeq2}, \mathrm{COeq3}, \mathrm{COeq4}, \mathrm{COeq(ave)}\right]. \tag{8}$$

- The EO will adjust the concentration in the third stage to achieve an appropriate balance between exploration and exploitation. The following formula is a description of the procedure for updating the EO formula:

$$\overrightarrow{\mathrm{CON}} = \overrightarrow{\mathrm{COeq}} + \left(\overrightarrow{\mathrm{CON}} - \overrightarrow{\mathrm{COeq}}\right) \times \vec{f} + \frac{\vec{g}}{\vec{\lambda} \times vo}\left(1 - \vec{f}\right). \tag{9}$$

Based on Eq. (9), $\overrightarrow{\mathrm{CON}}$ stands for the adjusted locations.

2.2.3 Adaptive neuro-fuzzy inference system (ANFIS)

Fuzzy systems and neural networks are combined in the ANFIS model. Jang's idea (Jang 1993) was used to address a variety of issues, notably forecasting and time series prediction. The "IF−THEN rules" are used in the ANFIS's fundamental framework to produce the "Takagi–Sugeno inference model," which generates input and output mappings.

Figure 4 depicts the fundamental organization of the ANFIS, with x and y standing in for Layer 1 inputs and L_{1i} for the node i's output. One definition of this is

$$L_{1i} = \mu_{A_i}(x),\ i = 1, 2,\ L_{1i} = \mu_{B_{i-2}}(y),\ i = 3, 4, \tag{10}$$

$$\mu(x) = e^{-\left(\frac{x-\rho_i}{\alpha_i}\right)^2}. \tag{11}$$

In these equations, A_i and B_i denote the membership values of the generalized Gaussian membership function, or μ, furthermore ρ_i and α_i stand for the premise variable set.

Layer 2's result is calculated as follows:

$$L_{2i} = \mu_{A_i}(x) \times \mu_{B_{i-2}}(y). \tag{12}$$

Layer 3's result is computed as follows:

$$L_{3i} = \overline{w_i} = \frac{\omega_i}{\sum_{(i=1)}^{2} \omega_i}. \tag{13}$$

In this equation, w_i stands for the ith result of layer number 2. Moreover, layer 4's result is determined as follows:

$$L_{4,i} = \overline{w_i} f_i = \overline{w_i}(p_i x + q_i y + r_i). \tag{14}$$

In the abovementioned equation, a function denoted by the f relies on the network's input and variables. In addition, the terms p_i, r_i, and q_i stand for the node I's subsequent variables.

Eventually, F and $\overline{w_i}$ (those stated in Eq. (13)), as described by Eq. (15), may be used to construct the result. Layer 5:

$$L_5 = \sum_i \overline{w_i} f_i. \tag{15}$$

In the ANFIS method, two essential factors are the steady and mean values of the input and output membership functions (Hussein 2016). Typically, gradient-based techniques are employed to adjust these parameters in ANFIS. However, a major drawback of these methods is that they often get stuck in local optima, resulting in slow convergence rates

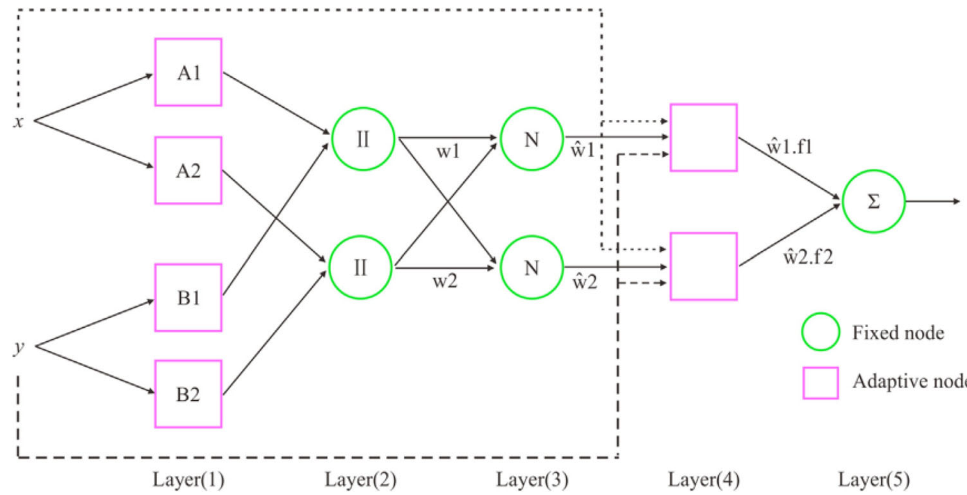

Fig. 4 Architecture schematics for ANFIS

(Bayat et al. 2019). To address this issue, optimization algorithms offer a valuable solution.

2.3 Performance indices

To evaluate the usefulness of ANAO, and ANEO systems, six metrics were computed and compared (Wu and Zhou 2023; Esmaeili-Falak and Sarkhani Benemaran 2023). The following metrics were computed as appropriate metrics to gain this objective (Eqs. (16–21)):

- Coefficient of determination (R^2)

$$R^2 = \left(\frac{\sum_{p=1}^{P} (t_P - \bar{t})(y_P - \bar{y})}{\sqrt{\left[\sum_{p=1}^{P} (t_P - \bar{t})^2\right]\left[\sum_{p=1}^{P} (y_P - \bar{y})^2\right]}} \right)^2. \tag{16}$$

- Root mean squared error (RMSE)

$$\text{RMSE} = \sqrt{\frac{1}{P}\sum_{p=1}^{P} \left(y_p - t_p\right)^2}. \tag{17}$$

- Mean absolute error (MAE)

$$\text{MAE} = \frac{1}{P}\sum_{p=1}^{P} \left|y_p - t_p\right|, \tag{18}$$

- $A_{20-\text{Index}}$

$$A_{\text{20-Index}} = \frac{m_{20}}{M}. \tag{19}$$

- Relative absolute error (RAE)

$$\text{RAE} = \frac{\sum_{p=1}^{P} \left|y_p - t_p\right|}{\sum_{p=1}^{P} \left|y_p - \bar{y}\right|}. \tag{20}$$

- Root relative squared error (RRSE)

$$\text{RRSE} = \sqrt{\frac{\sum_{p=1}^{P} (y_p - t_p)^2}{\sum_{p=1}^{P} (y_p - \bar{y})^2}}, \tag{21}$$

where, correspondingly, y_P, t_P, $\bar{t}$, and $\bar{y}$ are the goal, forecasted values, and the mean of the goal and forecasted of them. Here, M is the sample count, and m_{20} is the sample count with Meas./Est. $= 0.8 - 1.2$.

3 Results and discussion

3.1 Development process

For modeling the ANAO and ANEO, a beginning ANFIS model was proposed for the initial stage; then, the AOA and EO algorithms were introduced for optimizing the developed ANFIS model. In this task, the variables of membership functions of the produced ANFIS were trained (optimized) using the optimization algorithms. Herein, RMSE was utilized as a fitness function to evaluate the accuracy of the optimization procedure for the ANAO and ANEO models. Finally, the optimum ANAO and ANEO models were determined with the number of fuzzy terms and the highest iterations, as shown in Table 2.

Table 2 Control parameters of algorithms

Method	Parameter	Value	Single and hybrid methods	Parameter description/value	Value
General	Number of runs	20	ANFIS	Number of inputs	8
	Population size	20		Number of outputs	1
	Max_Num_Iterations	200		Fuzzy structure	$Sugeno$
				Initial FIS for training	$genfis2$
				Membership function type	$Dsigmf$
				Output membership function	Linear
				Optimization method	Hybrid
				Step size decrease rate	0.1
				Step size increase rate	1
AOA	C_{iter}	1	ANAO	Number of fuzzy terms	22
	$\text{MOP}_{\min}$	0.2		The highest iterations	30
	$\text{MOP}_{\max}$	1			
	α	5			
	μ	0.499			
EO	α_1	2	ANEO	Number of fuzzy terms	15
	α_2	1		The highest iterations	30
	GP	0.5			

3.2 Analysis

This paper presents the results of the single ANFIS and hybrid ANAO and ANEO designs in order to forecast the CS of the HPC system enhanced with BFS and FA. By combining the crucial elements in the appropriate ratios, as mentioned earlier, the performance of ANFIS can be improved. The training and testing phases of the generated ANAO and ANEO systems are depicted in Fig. 5, illustrating the observed and calculated values of the CS of the HPC. Furthermore, when the percentage error in CS concentration is plotted on a graph, a bell-shaped distribution of curves is observed, with the central point of the distribution aligning with the zero-error percentage line. The effectiveness of the single ANFIS and hybrid ANAO and ANEO in making accurate forecasts of HPC's CS was evaluated using various metrics, including R^2, RMSE, MAE, RAE, RRSE and $A_{20\text{-Index}}$ (refer to Table 3). The results indicate that both ANAO and ANEO show great potential in delivering precise forecasts of HPC's CS compared to single ANFIS.

One aspect of this study focuses on evaluating the efficacy of multiple iterations of the statistical identifiers (ANFIS, ANAO, and ANEO) developed for the published studies. The findings of this inquiry were also subject to objective evaluation in comparison to other published studies. The results indicate that the combined ANAO and ANEO systems demonstrated strong estimation capabilities, with R^2 values of 0.9941 and 0.9975 for the training and testing components of ANAO, and 0.9878 and 0.9929 for ANEO, respectively. In order to identify the optimal approach, it is essential to examine and evaluate the generated signals thoroughly. When comparing the ANEO, it was observed that the ANAO RMSE value decreased during training, decreasing from 1.9571 to 1.3588 MPa. The testing results indicated a modest decline from 1.1351 to 0.6662 MPa. Likewise, the MAE, RAE, and RRSE metrics yielded consistent results as the RMSE, indicating that the ANAO exhibited greater proficiency in CS estimation. The RRSE values further supported this, with the ANAO achieving 0.0767 MPa for $\text{RRSE}_{\text{Train}}$ and 0.0496 MPa for $\text{RRSE}_{\text{Test}}$, which were lower compared to the ANEO's values of 0.1105 MPa for $\text{RRSE}_{\text{Train}}$ and 0.0845 MPa for $\text{RRSE}_{\text{Test}}$. Similar outcomes were observed for the $A_{20-\text{Index}}$ signal, with a roughly 2% increase in both the training and testing sections for ANAO. The analysis of ANFIS by itself as well depicts acceptable performance, where its effectiveness was improved by linking with optimization algorithms.

The estimates provided here were developed after comparing several different methods, including Gene Expression Programming (GEP) (Mousavi et al. 2012), Semi-Empirical Method (SEM) (Nguyen et al. 2021b), Gaussian Process Regression (GPR) (Dao et al. 2020), artificial neural networks (ANN) (Chou and Pham 2013), Multi-Gene Genetic Programming (MGGP) (Gandomi and Alavi 2012), and Extreme Gradient Boosting (XGB) (Lee et al. 2022). Upon examining the table, it becomes evident that our proposed ANAO outperformed the previous studies documented in the literature. SEM (Nguyen et al. 2021b) performed poorly

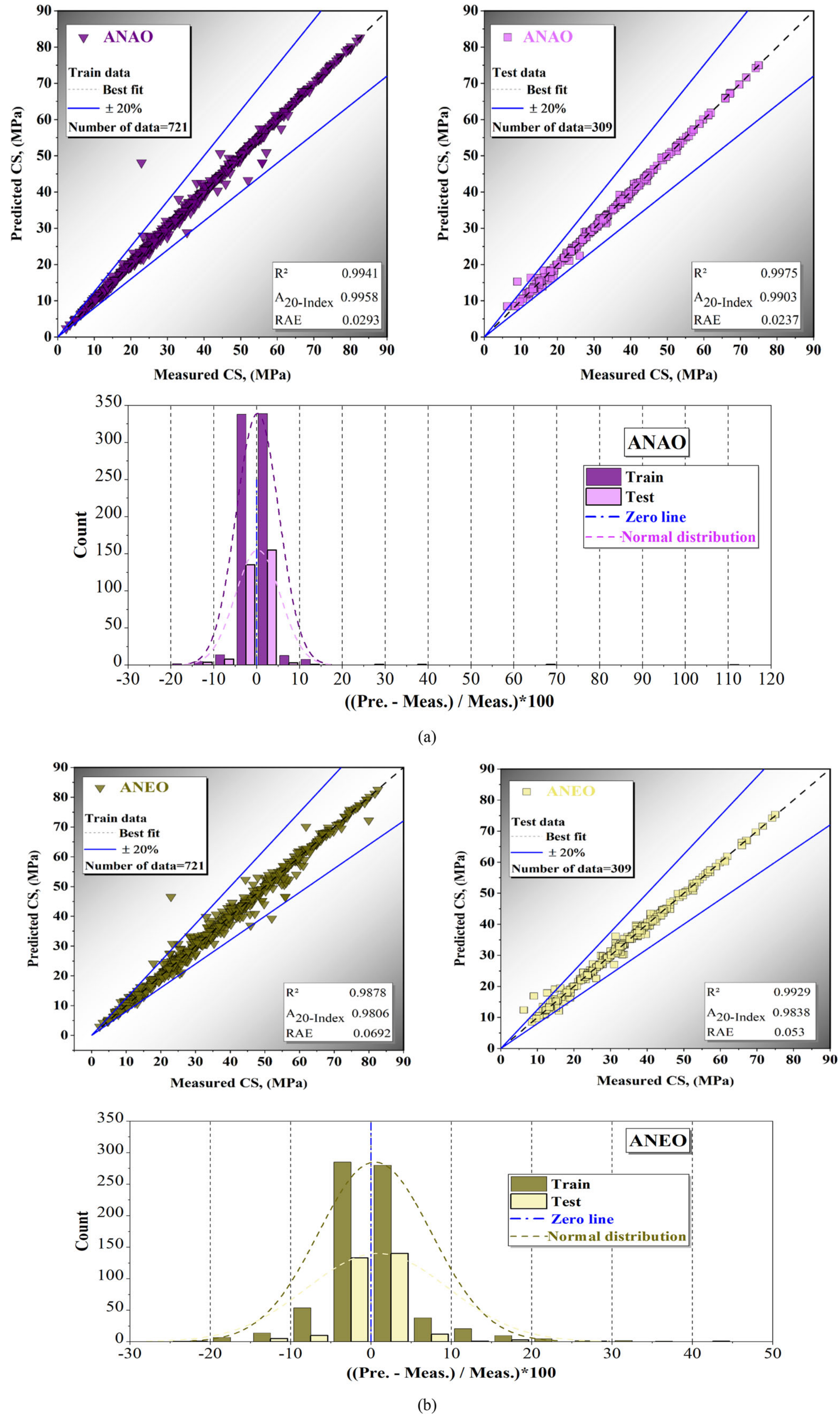

Fig. 5 The conclusions of the ANFIS models, **a** ANAO, **b** ANEO

Table 3 Performance of the created models

Stage	Index	This paper	This paper	This paper	Comparison with literature						
					Mousavi et al. 2012	Gandomi and Alavi 2012	Asteris et al. 2021	Chou and Pham 2013	Nguyen et al. 2021b	Dao et al. 2020	Lee et al. 2022
		ANFIS	ANAO	ANEO	GEP	MGGP	GPR	ANNs	SEM	GPR	XGB (all data)
Train	R^2	0.9626	0.9941	0.9878	0.8224	0.7885	0.987		0.84	0.888	0.944
	MAE (MPa)	2.0235	0.4255	1.0033	5.202	5.56			4.91	3.996	2.592
	RMSE (MPa)	3.428	1.3588	1.9571		7.36			6.3	5.59	3.878
	$A_{20\text{-Index}}$	0.9601	0.9958	0.9806			0.9753		0.68		
	RAE(MPa)	0.0986	0.0293	0.0692							
	RRSE (MPa)	0.3701	0.0767	0.1105							
Test	R^2	0.9713	0.9975	0.9929	0.8354	0.8046	0.8858	0.8649	0.8567	0.888	
	MAE (MPa)	1.012	0.2505	0.5613	5.19	5.48		4.421	4.482	3.913	
	RMSE (MPa)	2.362	0.6662	1.1351		7.31		6.329	5.968	5.597	
	$A_{20-\text{Index}}$	0.9625	0.9903	0.9838			0.757		0.752		
	RAE(MPa)	0.0868	0.0237	0.053							
	RRSE (MPa)	0.2586	0.0496	0.0845							

when compared to ANAO, with R^2 of 0.84 vs 0.9941, RMSE of 6.3 MPa vs 1.3588 MPa, MAE of 4.91 MPa vs 0.4255 MPa, and $A_{20-\text{Index}}$ of 0.68 vs 0.9958 MPa. For example, GEP (Mousavi et al. 2012) demonstrated a much higher MAE and a slightly lower R^2 when compared to ANAO (by 0.8224 and 5.202, respectively). The newest technique, XGB (Lee et al. 2022), came close to overtaking ANAO but eventually fell short. Other techniques, such MGGP (Gandomi and Alavi 2012) and ANNs (Chou and Pham 2013), performed worse than ANAO, with R^2 values that are much lower than 0.9862, at 0.8046 and 0.8469, respectively. The ANAO also outperformed the GPR in terms of R^2, RMSE, and MAE (Nguyen et al. 2021a). The ANAO structure, which was first created to represent HPC's CS and improved with FA and BFS, is recommended for usage in this situation.

While the research described in the paper shows promising results in predicting the compressive strength of high-performance concrete (HPC) containing fly ash and blast furnace slag using machine learning techniques, there are several remaining issues that need to be addressed before its practical application.

The study used additional components such as fly ash and blast furnace slag, but the practical application may involve HPC mixtures with varying types and proportions of supplementary materials. The model needs to be validated for different combinations of ingredients and proportions to ascertain its effectiveness across a wide range of HPC mixtures. The model should be tested for its ability to predict compressive strength not only for the specific HPC mixtures used in the study but also for new and untested mixtures or conditions that may not be well-represented in the training dataset.

Practical implementation of the model requires assessing the cost–benefit trade-offs associated with using machine learning predictions compared to traditional testing methods. A thorough cost–benefit analysis can help justify the adoption of the proposed model in real-world scenarios.

HPC structures are often designed for long-term use, and their performance over time is critical. The research might have focused on predicting compressive strength at a particular point in time. However, the practical application of the model would require understanding how the HPC's properties and strength evolve over extended periods, considering factors such as aging, environmental exposure, and durability.

4 Conclusions

The primary objective of this study is to present a practical approach for a comprehensive evaluation of machine learning algorithms in predicting the CS of HPC. The study focuses on utilizing the single and hybrid ANFIS models to develop models for predicting HPC characteristics. Notably, this research introduces novelty through the application of the AOA and EO, the evaluation of HPC with additional components, the comparison with prior literature, and the utilization of a large dataset with multiple input variables. These aspects contribute to advancing the understanding of predicting mechanical properties in HPC and provide a fresh approach for optimizing the performance of predictive models.

- The results indicate that the combined ANAO and ANEO systems demonstrated strong estimation capabilities, with R^2 values of 0.9941 and 0.9975 for the training and testing components of ANAO, and 0.9878 and 0.9929 for ANEO, respectively.
- When comparing the ANEO, it was observed that the ANAO RMSE value decreased during training, decreasing from 1.9571 to 1.3588 MPa. The testing results indicated a modest decline from 1.1351 to 0.6662 MPa. Likewise, the MAE, RAE, and RRSE metrics yielded that the ANAO exhibited greater proficiency in CS estimation. The RRSE values further supported this, with the ANAO achieving 0.0767 MPa for $RRSE_{Train}$ and 0.0496 MPa for $RRSE_{Test}$, which were lower compared to the ANEO's values of 0.1105 MPa for $RRSE_{Train}$ and 0.0845 MPa for $RRSE_{Test}$. Similar outcomes were observed for the $A_{20-\mathrm{Index}}$ signal, with a roughly 2% increase in both the training and testing sections for ANAO.
- The results comparison of this study with the literature presents the comprehensiveness and reliability of the created ANFIS model optimized with AOA for predicting the HPC's CS improved with FA and BFS, which could be applicable for practical usages.
- The type and number of parameters play a crucial role in constructing algorithms frameworks. By gathering additional data from various initiatives, it becomes possible to reduce limitations on future studies and gain a clearer understanding of the adaptability of the models used to evaluate the CS. The concept of employing innovative optimization approaches to improve the performance of computational models leads to the creation of a distinct generation of models that can be applied in diverse contexts. In this research, an AOA and EO techniques were employed to optimize the structure of the basic ANFIS model. Each optimization strategy contains unique and practical elements that require parametric analysis to achieve the optimal condition. Therefore, by utilizing different optimization methods, it becomes possible to eliminate this constraint.

Author contributions ZN: writing—original draft preparation, conceptualization, supervision, project administration. YY: methodology, software, validation, formal analysis. JS: language review, formal analysis, software, validation.

Declarations

Conflict of interest The authors declare no competing of interests.

References

Abualigah L, Diabat A, Mirjalili S, Abd Elaziz M, Gandomi AH (2021) The arithmetic optimization algorithm. Comput Methods Appl Mech Eng 376:113609. https://doi.org/10.1016/j.cma.2020.113609

Aghayari Hir M, Zaheri M, Rahimzadeh N (2022) Prediction of rural travel demand by spatial regression and artificial neural network methods (Tabriz County). J Transp Res

Akkurt S, Tayfur G, Can S (2004) Fuzzy logic model for the prediction of cement compressive strength. Cem Concr Res 34:1429–1433

Anyaoha U, Zaji A, Liu Z (2020) Soft computing in estimating the compressive strength for high-performance concrete via concrete composition appraisal. Constr Build Mater 257:119472

Asteris PG, Skentou AD, Bardhan A, Samui P, Pilakoutas K (2021) Predicting concrete compressive strength using hybrid ensembling of surrogate machine learning models. Cem Concr Res 145:106449

Atici U (2011) Prediction of the strength of mineral admixture concrete using multivariable regression analysis and an artificial neural network. Expert Syst Appl 38:9609–9618

Bayat S, Pishkenari HN, Salarieh H (2019) Observer design for a nano-positioning system using neural, fuzzy and ANFIS networks. Mechatronics 59:10–24

Baykasoğlu A, Dereli T, Tanış S (2004) Prediction of cement strength using soft computing techniques. Cem Concr Res 34:2083–2090

Benemaran RS (2023) Application of extreme gradient boosting method for evaluating the properties of episodic failure of borehole breakout. Geoenergy Sci Eng 226:211837

Bhanja S, Sengupta B (2002) Investigations on the compressive strength of silica fume concrete using statistical methods. Cem Concr Res 32:1391–1394

Bharatkumar BH, Narayanan R, Raghuprasad BK, Ramachandramurthy DS (2001) Mix proportioning of high performance concrete. Cem Concr Compos 23:71–80

Chen CLP, Liu Z, Feng S (2018) Universal approximation capability of broad learning system and its structural variations. IEEE Trans Neural Netw Learn Syst 30:1191–1204

Chopra P, Sharma RK, Kumar M (2016) Prediction of compressive strength of concrete using artificial neural network and genetic programming. Adv Mater Sci Eng 1:1–12

Chou J-S, Pham A-D (2013) Enhanced artificial intelligence for ensemble approach to predicting high performance concrete compressive strength. Constr Build Mater 49:554–563

Chou J-S, Tsai C-F (2012) Concrete compressive strength analysis using a combined classification and regression technique. Autom Constr 24:52–60

Chou J-S, Chong WK, Bui D-K (2016) Nature-inspired metaheuristic regression system: programming and implementation for civil engineering applications. J Comput Civ Eng 30:4016007

Dawei BRY, Bing Z, Bingbing G, Xibo G, Razzaghzadeh B (2023) Predicting the CPT-based pile set-up parameters using HHO-RF and PSO-RF hybrid models. Struct Eng Mech 86:673–686

del Campo I, Basterretxea K, Echanobe J, Bosque G, Doctor F (2011) A system-on-chip development of a neuro-fuzzy embedded agent for ambient-intelligence environments. IEEE Trans Syst Man Cybern Part B 42:501–512

Esmaeili-Falak M, Hajialilue-Bonab M (2012) Numerical studying the effects of gradient degree on slope stability analysis using limit equilibrium and finite element methods. Int J Acad Res 4:216–222. https://doi.org/10.7813/2075-4124.2012/4-4/A.30

Esmaeili-Falak M, Sarkhani Benemaran R (2023) Ensemble deep learning-based models to predict the resilient modulus of modified base materials subjected to wet-dry cycles. Geomech Eng 32:583–600

Esmaeili-Falak M, Katebi H, Javadi A (2018) Experimental study of the mechanical behavior of frozen soils—a case study of tabriz subway. Period Polytech Civ Eng 62:117–125

Esmaeili-Falak M, Katebi H, Vadiati M, Adamowski J (2019) Predicting triaxial compressive strength and Young's modulus of frozen sand using artificial intelligence methods. J Cold Reg Eng 33:4019007. https://doi.org/10.1061/(ASCE)CR.1943-5495.0000188

Faramarzi A, Heidarinejad M, Stephens B, Mirjalili S (2020) Equilibrium optimizer: a novel optimization algorithm. Knowl-Based Syst 191:105190. https://doi.org/10.1016/j.knosys.2019.105190

Gandomi AH, Alavi AH (2012) A new multi-gene genetic programming approach to nonlinear system modelling. Part I: materials and structural engineering problems. Neural Comput Appl 21:171–187

Han Q, Gui C, Xu J, Lacidogna G (2019) A generalized method to predict the compressive strength of high-performance concrete by improved random forest algorithm. Constr Build Mater 226:734–742

Hussein AM (2016) Adaptive neuro-fuzzy inference system of friction factor and heat transfer nanofluid turbulent flow in a heated tube. Case Stud Therm Eng 8:94–104

Jang J-SR (1993) ANFIS: adaptive-network-based fuzzy inference system. IEEE Trans Syst Man Cybern 23:665–685. https://doi.org/10.1109/21.256541

Kasperkiewicz J, Racz J, Dubrawski A (1995) HPC strength prediction using artificial neural network. J Comput Civ Eng 9:279–284

Khorsheed MS, Al-Thubaity AO (2013) Comparative evaluation of text classification techniques using a large diverse Arabic dataset. Lang Resour Eval 47:513–538

Lai S, Serra M (1997) Concrete strength prediction by means of neural network. Constr Build Mater 11:93–98

Le-Duc T, Nguyen Q-H, Nguyen-Xuan H (2020) Balancing composite motion optimization. Inf Sci (NY) 520:250–270

Lee S-C (2003) Prediction of concrete strength using artificial neural networks. Eng Struct 25:849–857

Lee S, Nguyen N, Karamanli A, Lee J, Vo TP (2022) Super learner machine-learning algorithms for compressive strength prediction of high performance concrete. Struct Concr 24(2):2208–2228

Leema N, Nehemiah HK, Kannan A (2016) Neural network classifier optimization using differential evolution with global information and back propagation algorithm for clinical datasets. Appl Soft Comput 49:834–844

Leung CKY (2001) Concrete as a building material. Encycl Mater Sci Technol 1:1471–1479

Masoumi F, Najjar-Ghabel S, Safarzadeh A, Sadaghat B (2020) Automatic calibration of the groundwater simulation model with high parameter dimensionality using sequential uncertainty fitting approach. Water Supply 20:3487–3501

Mittal A, Sharma S, Kanungo DP (2012) A comparison of ANFIS and ANN for the prediction of peak ground acceleration in Indian Himalayan region. In: Proc. int. conf. soft comput. probl. solving (SocProS 2011) December 20–22, 2011, vol 2. Springer, pp 485–495

Moradi G, Hassankhani E, Halabian AM (2020) Experimental and numerical analyses of buried box culverts in trenches using geofoam. Proc Inst Civil Eng-Geotech Eng 175(3):311–322

Mousavi SM, Aminian P, Gandomi AH, Alavi AH, Bolandi H (2012) A new predictive model for compressive strength of HPC using gene expression programming. Adv Eng Softw 45:105–114

Najafzadeh M, Azamathulla HM (2015) Neuro-fuzzy GMDH to predict the Scour Pile Groups due to waves. J Comput Civ Eng 29:04014068. https://doi.org/10.1061/(ASCE)CP.1943-5487.0000376

Najafzadeh M, Saberi-Movahed F (2019) GMDH-GEP to predict free span expansion rates below pipelines under waves. Mar Georesour Geotechnol 37:375–392

Najafzadeh M, Saberi-Movahed F, Sarkamaryan S (2018) NF-GMDH-based self-organized systems to predict bridge pier scour depth under debris flow effects. Mar Georesour Geotechnol 36:589–602

Namyong J, Sangchun Y, Hongbum C (2004) Prediction of compressive strength of in-situ concrete based on mixture proportions. J Asian Archit Build Eng 3:9–16

Neville A, Aitcin P-C (1998) High performance concrete—an overview. Mater Struct 31:111–117

Nguyen H, Vu T, Vo TP, Thai H-T (2021a) Efficient machine learning models for prediction of concrete strengths. Constr Build Mater 266:120950

Nguyen N-H, Vo TP, Lee S, Asteris PG (2021b) Heuristic algorithm-based semi-empirical formulas for estimating the compressive strength of the normal and high performance concrete. Constr Build Mater 304:124467

Pala M, Özbay E, Öztaş A, Yuce MI (2007) Appraisal of long-term effects of fly ash and silica fume on compressive strength of concrete by neural networks. Constr Build Mater 21:384–394

Rafiei MH, Khushefati WH, Demirboga R, Adeli H (2017) Supervised deep restricted Boltzmann machine for estimation of concrete. ACI Mater J 114:237

Sarıdemir M (2009) Predicting the compressive strength of mortars containing metakaolin by artificial neural networks and fuzzy logic. Adv Eng Softw 40:920–927

Sarkhani Benemaran R, Esmaeili-Falak M, Katebi H (2020) Physical and numerical modelling of pile-stabilised saturated layered slopes. Proc Inst Civ Eng Eng. https://doi.org/10.1680/jgeen.20.00152

Sarkhani Benemaran R, Esmaeili-Falak M, Javadi A (2022) Predicting resilient modulus of flexible pavement foundation using extreme gradient boosting based optimised models. Int J Pavement Eng. https://doi.org/10.1080/10298436.2022.2095385

Topcu IB, Sarıdemir M (2008) Prediction of compressive strength of concrete containing fly ash using artificial neural networks and fuzzy logic. Comput Mater Sci 41:305–311

Van Dao D, Adeli H, Ly H-B, Le LM, Le VM, Le T-T, Pham BT (2020) A sensitivity and robustness analysis of GPR and ANN for high-performance concrete compressive strength prediction using a Monte Carlo simulation. Sustainability 12:830

Wu Y, Zhou Y (2022a) Splitting tensile strength prediction of sustainable high-performance concrete using machine learning techniques. Environ Sci Pollut Res 29:89198–89209

Wu Y, Zhou Y (2022b) Hybrid machine learning model and Shapley additive explanations for compressive strength of sustainable concrete. Constr Build Mater 330:127298

Wu Y, Zhou Y (2023) Prediction and feature analysis of punching shear strength of two-way reinforced concrete slabs using optimized machine learning algorithm and Shapley additive explanations. Mech Adv Mater Struct 30:3086–3096

Yan K, Shi C (2010) Prediction of elastic modulus of normal and high strength concrete by support vector machine. Constr Build Mater 24:1479–1485. https://doi.org/10.1016/j.conbuildmat.2010.01.006

Yeh I-C (1998a) Modeling of strength of high-performance concrete using artificial neural networks. Cem Concr Res 28:1797–1808

Yeh I-C (1998b) Modeling concrete strength with augment-neuron networks. J Mater Civ Eng 10:263–268

Yeh I-C (1999) Design of high-performance concrete mixture using neural networks and nonlinear programming. J Comput Civ Eng 13:36–42

Yeh I-C (2003) Prediction of strength of fly ash and slag concrete by the use of artificial neural networks. J Chin Inst Civ Hydraul Eng 15:659–663

Yeh I-C (2006) Analysis of strength of concrete using design of experiments and neural networks. J Mater Civ Eng 18:597–604

Yeh I-C, Lien L-C (2009) Knowledge discovery of concrete material using genetic operation trees. Expert Syst Appl 36:5807–5812

Young BA, Hall A, Pilon L, Gupta P, Sant G (2019) Can the compressive strength of concrete be estimated from knowledge of the mixture proportions?: new insights from statistical analysis and machine learning methods. Cem Concr Res 115:379–388

Zain MFM, Abd SM (2009) Multiple regression model for compressive strength prediction of high performance concrete. J Appl Sci 9:155–160

Zarandi MHF, Türksen IB, Sobhani J, Ramezanianpour AA (2008) Fuzzy polynomial neural networks for approximation of the compressive strength of concrete. Appl Soft Comput 8:488–498

Zhu Y, Huang L, Zhang Z, Bayrami B (2022) Estimation of splitting tensile strength of modified recycled aggregate concrete using hybrid algorithms. Steel Compos Struct 44:389–406